Thermodynamics of Denaturation of Barstar: Evidence for Cold Denaturation and Evaluation of the Interaction with Guanidine Hydrochloride†

Vishwas R. Agashe and Jayant B. Udgaonkar*

National Centre for Biological Sciences, TIFR Centre, P.O. Box 1234, Indian Institute of Science Campus, Bangalore 560012, India

Received October 17, 1994; Revised Manuscript Received December 19, 1994®

ABSTRACT: Isothermal guanidine hydrochloride (GdnHCl)-induced denaturation curves obtained at 14 different temperatures in the range 273−323 K have been used in conjunction with thermally-induced denaturation curves obtained in the presence of 15 different concentrations of GdnHCl to characterize the thermodynamics of cold and heat denaturation of barstar. The linear free energy model has been used to determine the excess changes in free energy, enthalpy, entropy, and heat capacity that occur on denaturation. The stability of barstar in water decreases as the temperature is decreased from 300 to 273 K. This decrease in stability is not accompanied by a change in structure as monitored by measurement of the mean residue ellipticities at both 222 and 275 nm. When GdnHCl is present at concentrations between 1.2 and 2.0 M, the decrease in stability with decrease in temperature is however so large that the protein undergoes cold denaturation. The structural transition accompanying the cold denaturation process has been monitored by measuring the mean residue ellipticity at 222 nm. The temperature dependence of the change in free energy, obtained in the presence of 10 different concentrations of GdnHCl in the range 0.2−2.0 M, shows a decrease in stability with a decrease as well as an increase in temperature from 300 K. Values of the thermodynamic parameters governing the cold and the heat denaturation of barstar have been obtained with high precision by analysis of these bell-shaped stability curves. The change in heat capacity accompanying the unfolding reaction, ΔC_P, has a value of 1460 ± 70 cal mol^{-1} K^{-1} in water. The dependencies of the changes in enthalpy, entropy, free energy, and heat capacity on GdnHCl concentration have been analyzed on the basis of the linear free energy model. The changes in enthalpy (ΔH_i) and entropy (ΔS_i), which occur on preferential binding of GdnHCl to the unfolded state, vis-a-vis the folded state, both have a negative value at low temperatures. With an increase in temperature ΔH_i makes a less favorable contribution, while ΔS_i makes a more favorable contribution to the change in free energy (ΔG_i) due to this interaction. The change in heat capacity (ΔC_{Pi}) that occurs on preferential interaction of GdnHCl with the unfolded form has a value of only 53 ± 36 cal mol^{-1} K^{-1} M^{-1}. The data validate the linear free energy model that is commonly used to analyze protein stability.

An accurate measurement of the stability of a protein, in terms of the free energy of unfolding (ΔG) is vital for a correct understanding of the physical interactions that stabilize the protein. The reliability of these measurements assumes importance in studies where the stabilizing interactions are perturbed either through mutagenesis of the amino acid sequence or through a change in environmental conditions. The stability estimate of a protein is very often based on the analysis of denaturant-induced or thermally-induced unfolding transitions, measured either spectroscopically or calorimetrically. In either case, it is necessary to extrapolate the free energy of unfolding to standard conditions, typically 298 K in the absence of denaturant. Extrapolation of thermally-induced transitions is possible if the change in heat capacity that accompanies unfolding is accurately known, and it is important to establish that this thermodynamic parameter is independent of temperature (Privalov *et al.*, 1989).

Extrapolation of urea or guanidine hydrochloride (GdnHCl)[1] induced denaturation curves is carried out using either the linear free energy model that has been theoretically rationalized by Schellman (1978, 1987) or the binding model rationalized by Tanford (1970). Although, the linear free energy model is by far the most commonly used model, there is surprisingly no report of studies that validate this model by predicting and accounting for all the thermodynamic parameters that define the model. Attempts to validate the linear free energy model have invariably relied on comparing extrapolations from thermally-induced and denaturant-induced unfolding curves (Pace, 1986; Becktel & Schellman, 1987). On the other hand, the most detailed study to date of the interaction of denaturants with proteins (Makhatadze & Privalov, 1992) appears to validate the binding model. Thus, it is evident that there is considerable debate about how chemical denaturants unfold proteins.

The choice of protein is an important factor in evaluating the physical interactions that determine its stability and also in correlating this evaluation with its structure. The protein

† This work was funded by the Tata Institute of Fundamental Research and the Department of Biotechnology, Government of India. J.B.U. is the recipient of a Biotechnology Career fellowship from the Rockefeller Foundation.

* Corresponding author; e-mail address: jayant@tifrbng.ernet.in or jayant@tifrvax.bitnet.

® Abstract published in *Advance ACS Abstracts,* February 15, 1995.

[1] NMR, nuclear magnetic resonance; CD, circular dichroism; GdnHCl, guanidine hydrochloride; DTT, dithiothreitol; EDTA, ethylenediaminetetraacetic acid.

0006-2960/95/0434-3286$09.00/0

must fold completely and reversibly, its three-dimensional structure must be known, it should be small enough for NMR studies, and it should have a good expression system for protein engineering studies. Barstar, the intracellular inhibitor of barnase in *Bacillus amyloliquefaciens*, is an attractive model protein for the study of protein folding (Hartley, 1988). This 89 amino acid residue protein comprises four α-helices and a parallel three-stranded β-sheet (Guillet *et al.*, 1993; Buckle *et al.*, 1994). Complete proton NMR assignments of the protein and a solution structure are available (Lubienski *et al.*, 1993, 1994; S. Ramachandran and J. B. Udgaonkar, unpublished results). Both barstar (Khurana & Udgaonkar, 1994; Swaminathan *et al.*, 1994) and a Cys48Cys82→Ala48Ala82 double mutant form of barstar (A. Hate and J. B. Udgaonkar, unpublished results) transform to a molten globule-like conformation at low pH, and kinetic studies (Schreiber & Fersht, 1993; Shastry *et al.*, 1994) have demonstrated the presence of multiple folding intermediates and at least three parallel folding pathways.

In this paper, it is demonstrated that the stability of barstar in water decreases as the temperature is lowered from 300 to 273 K at pH 8, where the protein possesses its functional structure. This decrease in stability is however not accompanied by a decrease in mean residue ellipticity at either 222 or 275 nm. In the presence of GdnHCl in the concentration range 1.2−2.0 M, the decrease in stability with a decrease in temperature is however so large that barstar undergoes cold denaturation. This is the first paper to describe the cold denaturation of barstar. The ability to study both cold and heat denaturation over a range of GdnHCl concentrations has made it possible to accurately determine the values of the thermodynamic parameters governing the unfolding of the protein and its interaction with GdnHCl using the linear free energy model (Schellman, 1978). A complete thermodynamic analysis of barstar over a wide range of both temperature and GdnHCl concentrations is presented here. The data validate the linear free energy model that is commonly used to analyze urea and GdnHCl-induced denaturation curves (Pace, 1986).

MATERIALS AND METHODS

Protein Purification. The plasmid encoding the gene for barstar (pMT316) was a generous gift from Dr. R. W. Hartley (1988) and was expressed in *Escherichia coli* strain MM294. The procedure for the purification of barstar has been described previously (Khurana & Udgaonkar, 1994).

Buffers and Solutions. All the experiments utilized buffers containing 2 mM buffer (sodium phosphate), 100 μM EDTA and 100 μM DTT at pH 8, and a variable concentration of GdnHCl in the range 0−6 M. The solutions were made by appropriate mixing of the acidic and basic forms of the buffer so as to obtain the desired final pH. The pH values of all solutions were carefully checked before use. All solutions were passed through 0.22-μm Corning filters and degassed before use. The concentrations of the GdnHCl stock solutions were determined by refractive index measurements (Pace *et al.*, 1989) on an Abbe refractometer. All chemicals used were of the highest purity grade.

GdnHCl-Induced Denaturation. Equilibrium unfolding as a function of GdnHCl concentration was monitored by far-UV CD and also by near-UV CD. CD measurements were done on a Jasco J720 spectropolarimeter. Spectra were collected with the slit width set to 430 μm, a response time of 4 s, and a scan speed of 20 nm/min. Each spectrum was the average of at least 10 scans. The number of scans was increased with an increase in the photomultiplier voltage that occurs with an increase in GdnHCl concentration. Secondary structure measurements were made at 222 nm with protein concentrations of 6 μM in a 0.3-cm path length cuvette obtained from Shimadzu Corporation, Japan. Near-UV measurements at 275 nm were done using a protein concentration of 40 μM with a cuvette of path length 1 cm obtained from Sigma. The sample temperature was maintained using a Neslab RTE-110 circulating water bath.

Thermal Denaturation. Thermal denaturation was followed by monitoring mean residue ellipticity either at 222 or 275 nm using a Jasco J720 spectropolarimeter interfaced to a Neslab RTE-110 circulating water bath. A cylindrical 2-mm water-jacketed cuvette obtained from Jasco was used for all experiments in the far-UV region, and the protein concentration employed was 10 μM. For near-UV CD melts, a 1-cm path length cuvette was used, and the protein concentration was 40 μM. The heating rate used was 0.33 K/min. Using half this heating rate yielded an identical denaturation curve. The temperature in the cuvette was monitored during measurement using a Thermolyne digital pyrometer. The accuracy of the probe was ±0.5 K. Special care was taken to keep the loss in volume of the protein solution due to evaporation to less than 3% of the initial volume.

Data Analysis. For a two-state N ⇌ U unfolding reaction characterized by a change in heat capacity, ΔC_P, which is independent of temperature in the range of measurements (Privalov, 1979), the thermodynamic equations for the dependence of the change in enthalpy (ΔH), entropy (ΔS), and free energy (ΔG) on temperature in the absence of any denaturant are well known:

$$\Delta G = \Delta H - T\Delta S \tag{1}$$

$$\Delta H(T) = \Delta H_g + \Delta C_P(T - T_g) \tag{2}$$

$$\Delta S(T) = \Delta S_g + \Delta C_P \ln(T/T_g) \tag{3}$$

$$\Delta G(T) = \Delta H_g\left(1 - \frac{T}{T_g}\right) + \Delta C_P(T - T_g - T\ln(T/T_g)) \tag{4}$$

T_g, the midpoint of the thermal transition, and therefore the temperature at which $\Delta G(T) = 0$, is taken as the standard reference temperature. ΔH_g and ΔS_g are the values of ΔH and ΔS at T_g.

According to the linear free energy model (Schellman, 1978, 1987; Chen & Schellman, 1989), the changes in free energy, enthalpy, entropy, and heat capacity that occur on unfolding in the presence of denaturant, denoted here by $\Delta G'$, $\Delta H'$, $\Delta S'$, and $\Delta C_P'$, respectively, all have a linear dependence on the concentration of denaturant [D]:

$$\Delta G' = \Delta G + m_G[D] = \Delta G + \Delta G_i[D] \tag{5}$$

$$\Delta H' = \Delta H + \Delta H_i[D] \tag{6}$$

$$\Delta S' = \Delta S + \Delta S_i[D] \quad (7)$$

$$\Delta C_P' = \Delta C_P + \Delta C_{Pi}[D] \quad (8)$$

$$\Delta G_i = \Delta H_i - T\Delta S_i \quad (9)$$

$$\Delta G' = \Delta H' - T\Delta S' \quad (10)$$

where m_G or ΔG_i, ΔH_i, ΔS_i, and ΔC_{Pi} are the changes in free energy, enthalpy, entropy, and heat capacity, respectively, associated with the preferential interaction of denaturant with the unfolded form of the protein relative to the folded form. The denaturant concentration at which the protein is half unfolded (when $\Delta G' = 0$) at any temperature T is given by C_m, and from eq 5, $\Delta G = -C_m m_G$.

With the assumption that ΔC_{Pi} is independent of temperature, the temperature dependencies of ΔH_i, ΔS_i, and ΔG_i are given by

$$\Delta H_i = \Delta H_i^\circ + \Delta C_{Pi}(T - T_o) \quad (11)$$

$$\Delta S_i = \Delta S_i^\circ + \Delta C_{Pi} \ln(T/T_o) \quad (12)$$

$$\Delta G_i(T) = \Delta H_i^\circ - T\Delta S_i^\circ + \Delta C_{Pi}(T - T_o - T \ln (T/T_o)) \quad (13)$$

where ΔH_i° and ΔS_i° are the values of ΔH_i and ΔS_i at a reference temperature T_o, which may for instance be set to T_g'. Thus, the temperature dependencies of $\Delta H'$, $\Delta S'$, and $\Delta G'$ are given by

$$\Delta H'(T) = \Delta H_g' + \Delta C_P'(T - T_g') \quad (14)$$

$$\Delta S'(T) = \Delta S_g' + \Delta C_P' \ln(T/T_g') \quad (15)$$

$$\Delta G'(T) = \Delta H_g'(1 - (T/T_g')) + \Delta C_P'(T - T_g' - T \ln (T/T_g')) \quad (16)$$

T_g', the midpoint of the thermal transition determined in the presence of GdnHCl, is the temperature at which $\Delta G'(T) = 0$.

Isothermal GdnHCl Denaturation Curves. A GdnHCl-induced denaturation curve determined at a temperature T was analyzed in two different but equivalent ways to obtain ΔG, the free energy of unfolding in water at temperature T.

In the first method of analysis, the equilibrium unfolding data were directly fitted to a two state F ⇌ U unfolding model, using eq 17 (Santoro & Bolen, 1988)

$$Y_O = \frac{Y_F + m_F[D] + (Y_U + m_U[D])\exp\left[\frac{-(\Delta G + m_G[D])}{RT}\right]}{1 + \exp\left[\frac{-(\Delta G + m_G[D])}{RT}\right]} \quad (17)$$

where Y_O is the value of the spectroscopic property being measured at denaturant concentration [D]. Y_F and Y_U represent the intercepts, and m_F and m_U are the slopes of the native and the unfolded baselines, respectively.

In the second method of analysis, the raw data were first converted to plots of f_U, the fraction of protein in the unfolded state versus [D] using eq 18:

$$f_U = \frac{Y_O - (Y_F + m_F[D])}{(Y_U + m_U[D]) - (Y_F + m_F[D])} \quad (18)$$

f_U is related to ΔG by a transformation of the Gibbs–Helmholtz equation in which the equilibrium constant for unfolding in the folding transition zone, K_{app}, is given by $K_{app} = f_U/(1 - f_U)$.

$$f_U = \frac{\exp\left[\frac{-(\Delta G + m_G[D])}{RT}\right]}{1 + \exp\left[\frac{-(\Delta G + m_G[D])}{RT}\right]} \quad (19)$$

Thermally-Induced Denaturation Curves. To obtain estimates for T_g' and $\Delta H_g'$, a thermal denaturation curve obtained in the absence or presence of GdnHCl was analyzed as follows: The apparent equilibrium constant K_{app} and the free energy change $\Delta G'$ at any temperature T within the folding transition zone of the thermally-induced transition were first determined from the raw data using the following equations:

$$K_{app} = \frac{f_U}{1 - f_U} = \frac{Y_O - (Y_F + m_F T)}{(Y_U + m_U T) - Y_O} \quad (20)$$

$$\Delta G' = -RT \ln K_{app} = -RT \ln \left(\frac{Y_O - (Y_F + m_F T)}{(Y_U + m_U T) - Y_O}\right) \quad (21)$$

where Y_O is the mean residue ellipticity measured at temperature T in the presence of denaturant at concentration [D], Y_F and Y_U represent the intercepts, and m_F and m_U are the slopes of the folded and the unfolded baselines of the data (see Results), respectively. f_U is the fraction of barstar in the unfolded form. Values of K_{app} well within the transition zone were used to obtain values of $\Delta G'$ as a function of T (in K), and T_g' was determined as the temperature at which $\Delta G' = 0$. The slope of a plot $\Delta G'$ versus T at T_g' is, according to eq 16, equal to $-\Delta H_g'/T_g'$, which represents $-\Delta S_g'$ the change in entropy accompanying the unfolding reaction at T_g'. Thus, $\Delta H_g'$ and $\Delta S_g'$ could be estimated. The value of $\Delta H_g'$ was also estimated from the slope of a van't Hoff plot ($\ln K_{app}$ versus $1/T$), which is equal to $-\Delta H_g'/R$. The two estimates for $\Delta H_g'$ so obtained were essentially identical.

Composite stability curves (Figure 6) were fit to eq 16 (for data obtained in the presence of GdnHCl) or eq 4 (for data obtained in the absence of GdnHCl) using the values obtained as described above as the starting estimates for T_g' and $\Delta H_g'$.

Thermal denaturation curves obtained in the presence of GdnHCl are described by

$$Y_O = \left\{(Y_F + m_F T) + (Y_U + m_U T) \times \exp\left[\frac{\Delta H_g'\left(\frac{T}{T_g'} - 1\right) + \Delta C_P'[T_g' - T + T \ln(T/T_g')]}{RT}\right]\right\} \Bigg/ 1 + \exp\left[\frac{\Delta H_g'\left(\frac{T}{T_g'} - 1\right) + \Delta C_P'[T_g' - T + T \ln(T/T_g')]}{RT}\right] \quad (22)$$

Thermally-induced denaturation data were also converted to plots of f_U (as defined in eq 18, with T replacing [D]), in which case they are described by equation 23:

$$f_U = \frac{\exp\left[\frac{\Delta H_g'\left(\frac{T}{T_g'} - 1\right) + \Delta C_P'[T_g' - T + T\ln(T/T_g')]}{RT}\right]}{1 + \exp\left[\frac{\Delta H_g'\left(\frac{T}{T_g'} - 1\right) + \Delta C_P'[T_g' - T + T\ln(T/T_g')]}{RT}\right]} \quad (23)$$

The equations used to describe a thermal denaturation curve obtained in the absence of GdnHCl have the same forms as eqs 22 and 23, but with ΔH_g and ΔC_P in place of $\Delta H_g'$ and $\Delta C_P'$.

The temperature dependence of the free energy of unfolding in the absence of GdnHCl has typical features described by the characteristic temperatures T_g, T_s, and T_h (Becktel & Schellman, 1987; Schellman, 1987), which are the temperatures at which ΔG, ΔS, and ΔH, respectively, are equal to zero. Thus, from eqs 2 and 3, these temperatures are related to each other by the following equations:

$$T_h = T_g - \frac{\Delta H_g}{\Delta C_P} \quad (24)$$

$$\ln(T_g/T_s) = \frac{\Delta H_g}{T_g \Delta C_P} \quad (25)$$

$$\Delta G_s = \Delta C_P(T_s - T_h) \quad (26)$$

The low-temperature melting point, the midpoint of the cold denaturation process, T_g^c can be estimated from the following equation, which is obtained by setting ΔG in eq 4 to 0 at T_g^c and expanding the logarithmic term in that equation as a series to the third power:

$$T_g^c \approx \frac{7T_g + \sqrt{49T_g^2 - 8T_g^2\left(\frac{6\Delta H_g}{T_g \Delta C_P} + 5\right)}}{2\left(\frac{6\Delta H_g}{T_g \Delta C_P} + 5\right)} \quad (27)$$

The equations describing the corresponding characteristic temperatures in the presence of GdnHCl (T_h', T_s', T_g', and $T_g^{c'}$) have the same forms as eqs 24–27, but with $\Delta H_g'$ and $\Delta C_P'$ in place of ΔH_g and ΔC_P. All data were analyzed using the SigmaPlot for Windows scientific graphing software.

RESULTS

Data Collection. Fourteen isothermal GdnHCl-induced equilibrium denaturation curves, in which the concentration of GdnHCl was incremented in units of 0.2 M in the range 0–5 M, were collected in the range of temperature between 273 and 323 K, at 3–4 K intervals. Fifteen thermally-induced equilibrium denaturation curves, in which the temperature was incremented in units of 2 K in the range 293–368 K, were collected in the presence of different concentrations of GdnHCl, in the range 0–4.2 M, at intervals of 0.2 M. Thermally-induced denaturation data were not collected below 293 K because of the long equilibration times involved, and isothermal GdnHCl-induced denaturation data were not collected above 323 K because the folded-protein baselines became too short for accurate analysis. The data were analyzed using eqs 1–27.

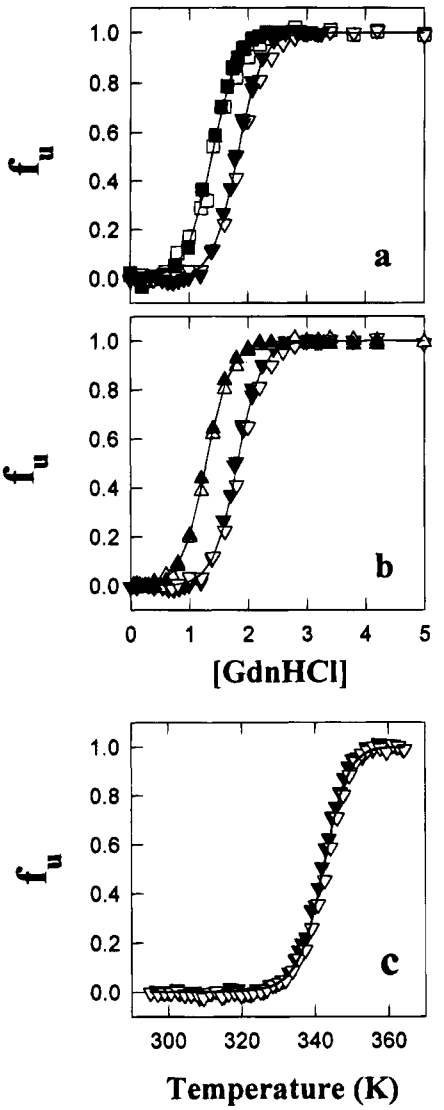

FIGURE 1: (a and b) GdnHCl-induced denaturation curves at three different temperatures at pH 8. The fraction of protein in the unfolded form (f_U), determined using eq 18, is plotted as a function of the concentration of GdnHCl at three different temperatures 277 (▲, △), 297 (▼, ▽), and 323 K (■, □). Open and closed symbols are from far-UV and near-UV CD experiments, respectively. The solid lines through the data are nonlinear least squares fits of the data to eq 19 and yield values for ΔG, C_m, and m_G of 3.4 ± 0.5 kcal mol^{-1}; 1.3 M, and 2.6 ± 0.2 kcal mol^{-1} M^{-1} at 277 K; 5.2 ± 0.5 kcal mol^{-1}, 1.8 M, and 2.9 ± 0.2 kcal mol^{-1} M^{-1} at 297 K; and 3.7 ± 0.5 kcal mol^{-1}, 1.4 M, and 2.7 ± 0.2 kcal mol^{-1} M^{-1} at 323 K. (c) Thermally-induced denaturation curve in the absence of GdnHCl at pH 8. Two probes were used, mean residue ellipticity at 222 (▼) and 275 nm (▽). The fraction of protein in the unfolded form, f_U, is plotted versus temperature. The raw data for the far-UV CD data are shown in Figure 3a. The solid line through the data is a nonlinear least squares fit according to eq 23, which yielded values for T_g, ΔH_g, and ΔC_P of 342.2 K, 67.2 kcal mol^{-1}, and 1410 kcal mol^{-1} K^{-1}, respectively.

Effect of Temperature on the Stability of Barstar. Figure 1, panels a and b, shows GdnHCl-induced denaturation curves for barstar at three different temperatures: 277, 297, and 323 K. Unfolding was monitored using two optical probes, far-UV CD at 222 nm and near-UV CD at 275 nm.

The former monitors secondary structure and the latter monitors tertiary structure. The mean residue ellipticity either at 222 or 275 nm, for barstar in the absence of GdnHCl, was the same at 277, 297, and 323 K. Data are plotted as f_U, the fraction of unfolded protein, versus the concentration of GdnHCl (see eq 18). Figure 1, panels a and b, shows that barstar is less stable at 277 and 323 K than at 297 K. Moreover, the transitions monitored by the two probes are coincident at all temperatures. For a given temperature, the same value of C_m, the midpoint of the unfolding transition, is obtained irrespective of the probe used. The good coincidence of the equilibrium unfolding profiles, as monitored by these two probes, is indicative of a two-state unfolding transition at each temperature. A fit of the data at each temperature to a two-state transition (eq 19) yields values for the three parameters that characterize the transition, namely, ΔG, C_m, and m_G (see legend to Figure 1 and also Figure 2). The value of C_m at 297 K is 1.8 ± 0.1 M, which is similar to the one reported earlier (Khurana & Udgaonkar, 1994; Shastry *et al.*, 1994).

In Figure 1c, the thermally-induced denaturation curves are shown for barstar in the absence of GdnHCl, monitored by two probes: mean residue ellipticity at 222 nm, a probe of secondary structure, and mean residue ellipticity at 275 nm, a probe of tertiary structure. Again, these two probes yielded coincident denaturation curves, described by eq 23, indicating that thermally-induced unfolding also proceeds through a two-state N ⇌ U transition.

Temperature Dependence of ΔG, m_G, and C_m. The 14 isothermal GdnHCl-induced denaturation curves determined in the temperature range 273−323 K were each analyzed using eq 17 to determine the values of the free energy change on unfolding in water, ΔG, the free energy of the interaction between barstar and GdnHCl, m_G (ΔG_i), and the midpoint of the GdnHCl-induced denaturation curve, C_m, at each temperature. The values of ΔG in the temperature range 341−351 K were also determined by the use of eq 21 from the thermal denaturation data collected in the absence of GdnHCl, which are shown in Figure 1c. The three thermodynamic parameters so determined are plotted versus absolute temperature in Figure 2. Figure 2a shows that ΔG decreases in value (i.e., the protein becomes less stable) when the temperature is either lowered or raised from 300 K. m_G appears to be independent of temperature, within experimental error, between 273 and 323 K, and has an average value of 2.4 ± 0.2 kcal mol^{-1} M^{-1}. C_m, which is less susceptible to experimental variation, has a dependence on temperature similar to that seen for ΔG in Figure 2a. Since m_G appears to be independent of temperature, within experimental error, the value of C_m can be justifiably used as an index of the stability of barstar.

The composite data in Figure 2a for the entire temperature range (273−363 K) were then fit to eq 4 to determine ΔH_g, ΔC_P, and T_g. Figure 2a shows that the data fit well to eq 4. The values obtained for ΔC_P, ΔH_g, and T_g are listed in Table 1.

Interconvertibility of GdnHCl and Temperature Melts. The equilibrium denaturation data collected from the 14 isothermal GdnHCl-induced unfolding experiments as well as the 15 thermally-induced unfolding experiments give the dependence of the mean residue ellipticity at 222 nm on both the temperature in the range 273−363 K, and the GdnHCl concentration in the range 0−5 M. Some of these data from

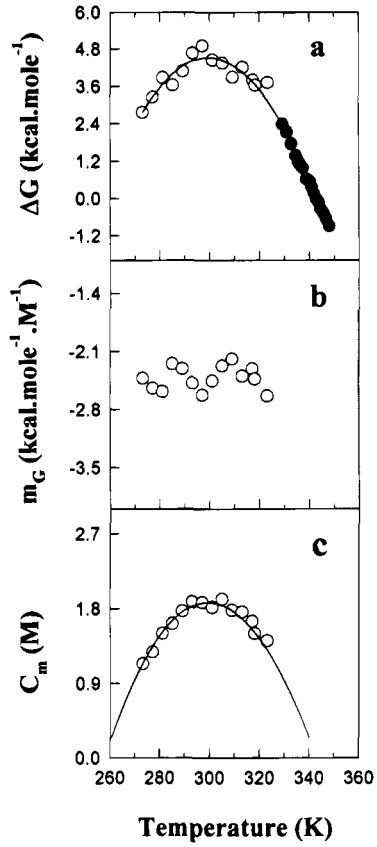

FIGURE 2: Temperature dependence of ΔG, m_G, and C_m. Open and closed symbols are used for data from isothermal GdnHCl-induced denaturation curves and thermally-induced denaturation curves, respectively. The solid line through the ΔG data (a) is a nonlinear least squares fit using eq 4. The values obtained for ΔH_g, T_g, and ΔC_P from the fit are listed in Table 1. The line through the C_m data (c) is drawn according to eq 4 and the relationship $C_m = -\Delta G/m_G$ (see text) with m_G set to −2.4 kcal mol^{-1} M^{-1}, which is its average value over the range in temperature indicated. The standard error in any value for ΔG and m_G obtained from an isothermal GdnHCl-induced denaturation curve, obtained from a nonlinear least squares fit of the curve to eq 17, was approximately ±6%, and the error bars fall within the size of the symbols. The standard error was lowest at T_s (300 K) and larger at both the low and high extremes of temperature, presumably because the folded-protein baselines were shorter at the extreme temperatures. The error in C_m was less than ±0.1 M as determined from multiple determinations of its value.

both sets of experiments are shown in Figure 3, panels a−d, where the mean residue ellipticity at 222 nm is plotted against temperature in the presence of different concentrations of GdnHCl. It is observed that the thermostability of the protein decreases with an increase in GdnHCl concentration: high-temperature unfolding occurs at lower temperatures, and low-temperature (cold) unfolding occurs at higher temperatures.

The data in Figure 3 exhibit several salient features. (1) There is very good coincidence between the data from GdnHCl-induced denaturation at fixed temperatures and the thermally-induced denaturation in the presence of fixed GdnHCl concentrations, when the former is transposed into the same form as the latter. This indicates that both sets of data have indeed been collected under true equilibrium conditions. (2) A global folded-protein baseline is drawn using the values of mean residue ellipticity at 222 nm in the temperature range 273−323 K, using measurements made in the presence of 0−1.0 M GdnHCl. A few points from the data obtained in the presence of 0.8 and 1.0 M GdnHCl,

Table 1: Thermodynamic Parameters Governing Thermally-Induced Denaturation of Barstar at pH 8.0[a]

[GdnHCl] (M)	T_g' (K)	$T_g^{c'}$ (K)	$\Delta H_g'$ (kcal mol^{-1})	$\Delta H_g^{c'}$ (kcal mol^{-1})	$\Delta S_g'$ (cal mol^{-1} K^{-1})	$\Delta S_g^{c'}$ (cal mol^{-1} K^{-1})	T_h' (K)	T_s' (K)	$\Delta G_s'$ (kcal mol^{-1})	$\Delta C_P'$ (cal mol^{-1} K^{-1})
0	343.0	257.8	69.7	−57.6	203.2	−223.4	296.3	299.4	4.5	1490
0.2	342.2	260.2	65.1	−54.2	190.2	−208.3	297.5	300.3	4.1	1460
0.4	340.3	261.6	58.4	−49.0	171.7	−187.3	297.5	300.1	3.5	1370
0.6	338.1	264.4	53.9	−45.8	159.4	−173.2	298.3	300.5	3.1	1350
0.8	335.5	267.6	49.4	−42.4	147.2	−158.4	299.0	300.9	2.6	1350
1.0	330.0	271.4	46.8	−41.1	141.8	−151.4	298.8	300.2	2.1	1500
1.2	326.1	274.9	41.2	−36.8	126.3	−133.9	299.1	300.2	1.7	1520
1.4	321.8	278.8	33.7	−30.7	104.7	−110.1	299.3	300.1	1.1	1500
1.6	316.5	283.9	25.4	−23.6	80.3	−83.1	299.6	300.1	0.7	1500
1.8	310.3	291.1	14.7	−14.1	47.4	−48.4	300.5	300.7	0.2	1500

[a] $\Delta H_g'$ and $\Delta S_g'$ are values calculated at temperature T_g', and $\Delta H_g^{c'}$ and $\Delta S_g^{c'}$ are values determined at temperature $T_g^{c'}$. T_g' and $T_g^{c'}$ were calculated from the stability curves (Figure 6) as described in the text. T_h' and T_s' were determined using eqs 24 and 25, respectively. Equation 26 was used to determine $\Delta G_s'$. Errors in the thermodynamic parameters are indicated in the text and figure legends.

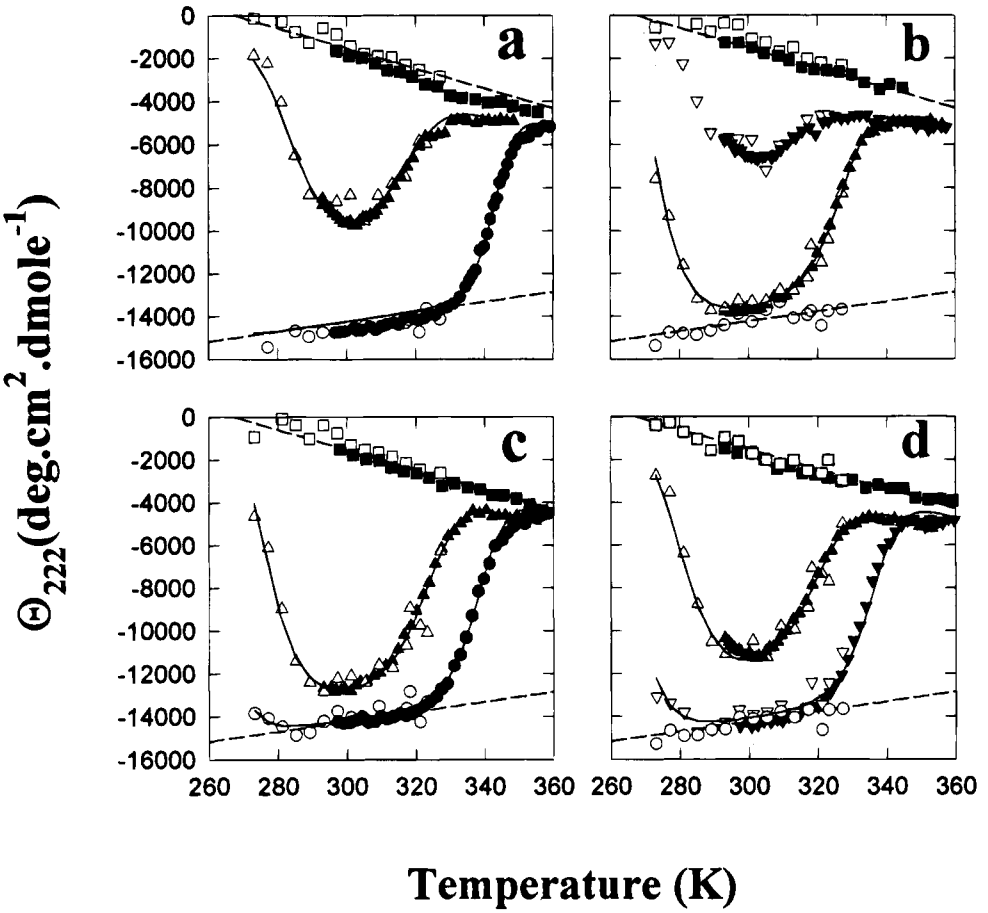

FIGURE 3: Temperature and GdnHCl concentration dependencies of the mean residue ellipticity at 222 nm. Open and closed symbols are from isothermal GdnHCl-induced and thermally-induced denaturation curves, respectively. The straight dashed lines at the top and bottom represent the global unfolded-protein baseline and the global folded-protein baseline, respectively. The former is a linear least-squares fit to all the data obtained in the presence of 2.6−5.0 M GdnHCl, while the latter is a linear least squares fit to all data obtained in the presence of 0−1 M GdnHCl. Different symbols indicate the different concentrations of GdnHCl present. (a) (○, ●) 0.0 M; (□, ■) 3.4 M; (△, ▲) 1.8 M. (b) (○) 0.3 M; (□, ■) 4.2 M; (△, ▲) 1.2 M; (▽, ▼) 2.0 M; (c) (○, ●) 0.6 M; (□, ■) 3.8 M; (△, ▲) 1.4 M. (d) (○) 0.1 M; (▽, ▼) 0.8 M; (□, ■) 3.0 M; (△, ▲) 1.6 M. Continuous lines through the data are simulated using eq 22 and the values for $\Delta H_G'$, T_g', and $\Delta C_P'$ listed in Table 1.

below 293 K were excluded from the fit for obtaining the global baseline as they were indicative of cold denaturation. Figure 3 demonstrates that the slope of the global folded-protein baseline is a good representative of the slopes of the individual folded-protein baselines that contribute to it, indicating that the temperature dependence of the mean residue ellipticity at 222 nm of the folded protein is virtually independent of GdnHCl in this narrow concentration range (0−1.0 M GdnHCl). The mean residue ellipticity of the folded protein decreases by less than 5% at 300 K, when the concentration of GdnHCl is increased from 0 to 1.0 M, the latter concentration being the highest concentration of GdnHCl in which the protein remains fully folded at this temperature. (3) A global unfolded-protein baseline could also be drawn in the temperature range 273−363 K, using measurements made in the presence of 2.6−5.0 M GdnHCl. Figure 3 demonstrates that the global unfolded-protein baseline is a good fit to these data over the entire temperature range, indicating that the temperature dependence of the mean residue ellipticity at 222 nm of the unfolded protein is

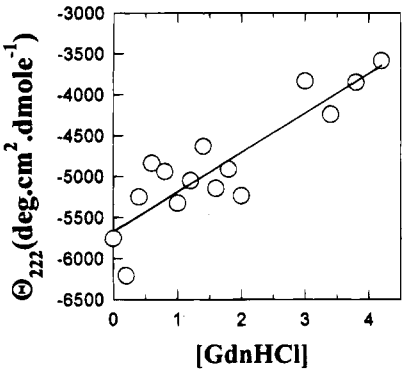

FIGURE 4: GdnHCl concentration dependence of the mean residue ellipticity at 222 nm at 349 K. The mean residue ellipticities at 222 nm and 349 K were obtained from thermal denaturation curves obtained in the presence of different concentrations of GdnHCl. The variation in the mean residue ellipticity was determined to be less than ±5% from multiple recordings of thermal denaturation curves. The straight line through the data is a linear least squares fit to the data and has a slope of 481° cm^{-2} dmol^{-1} M^{-1}.

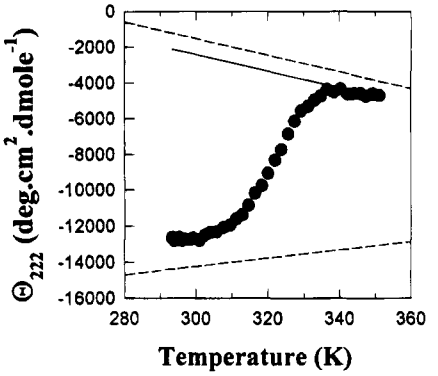

FIGURE 5: Analysis of a thermally-induced denaturation curve. The thermal denaturation experiment was done in the presence of 1.4 M GdnHCl at pH 8. The dashed lines represent the global folding and unfolding baselines as defined in the text. The upper solid line is the unfolding baseline used in the analysis and is a straight line drawn with the same slope as that of the global unfolding baseline, through the observed post-transition data points.

independent of GdnHCl concentration. (4) In the temperature range of measurement and at concentrations of GdnHCl between 0 and 1.0 M, barstar shows only one structural unfolding transition, that at high temperatures. (5) In the presence of an intermediate concentration of GdnHCl, between 1.2 and 2.0 M, barstar shows two structural unfolding transitions, one at a low temperature and the other at a high temperature. The magnitudes and midpoints of these transitions depend on the concentration of GdnHCl present. In this concentration range of GdnHCl, barstar is not fully folded at any temperature. (6) At GdnHCl concentrations above 2.6 M, no significant phase transition is observed. (7) The observed individual unfolded-protein baselines determined in the presence of 0−2.0 M GdnHCl do not coincide with the global unfolded-protein baseline. (8) The combination of data from both the isothermal GdnHCl-induced melts and the thermally-induced melts (which was possible because the data were coincident over the temperature range where they overlapped), resulting in composite temperature melts, allows the determination of thermodynamic parameters over the entire temperature range of 273−363 K. (9) The data collected in the presence of 2.0 M GdnHCl also show a good coincidence from the two sets of melts but fail to fit satisfactorily to the parameters obtained from a fit of the calculated $\Delta G'$ values to eq 16. There is a larger experimental error in the determination of the unfolded-protein baseline for the 2.0 M data, and this could account for the discrepancy. This kind of discrepancy has been reported before in the case of a mutant form of phage T4 lysozyme (Chen & Schellman, 1989), where it was similarly explained. In view of this inadequacy of the 2.0 M data, it was excluded from all further analysis.

GdnHCl Concentration Dependence of Mean Residue Ellipticity at 222 nm of Thermally Denatured Barstar. Figure 4 shows the dependence of the mean residue ellipticity at 222 nm on GdnHCl concentration at 349 K. At this temperature, the thermal transition is complete in the presence of any concentration of GdnHCl (Figure 3), and Figure 4 therefore illustrates the GdnHCl dependence of the mean residue ellipticity of thermally-denatured barstar. No cooperative transition is visible, and the mean residue ellipticity decreases linearly with an increase in GdnHCl concentration from 0 to 5.0 M.

Unfolded-Protein Baselines. The temperature dependence of the mean residue ellipticity at 222 nm of GdnHCl unfolded barstar (the global unfolded-protein baseline in Figure 3) and the GdnHCl concentration dependence of the mean residue ellipticity at 222 nm of thermally unfolded barstar (Figure 4) indicate that the individual unfolded-protein baseline for each thermal denaturation curve should be parallel to the global unfolded-protein baseline. Thus, for all thermal denaturation curves, individual unfolded-protein baselines were used as illustrated in Figure 5, which shows the individual unfolded-protein baseline used for the thermal denaturation curve in the presence of 1.4 M GdnHCl. Moving the point of intersection of the individual baseline with respect to the observed data in the post-transition zone had no significant effect on the values obtained for T_g', $\Delta H_g'$, and $\Delta C_P'$ after analysis (see below) as long as the slope of the global unfolded-protein baseline was used. As an extreme example, using the global unfolded-protein baseline instead of the individual unfolded-protein baseline shown alters the value of T_g' by less than 0.5 K and the values of $\Delta H_g'$ and $\Delta C_P'$ by less than 5%. This is true for all the thermal denaturation curves whose analyses are summarized in Table 1. For a composite thermal denaturation curve obtained in the presence of any GdnHCl concentration between 0 and 1.0 M, the individual observed folded-protein baseline was used for analysis. For the composite thermal denaturation curves obtained using GdnHCl concentrations between 1.2 and 2.0 M, the global folded-protein baseline was, however, used for analysis, because the protein was not completely folded at any temperature, and no individual folded-protein baseline was therefore observed (see Figure 3).

Analysis of Stability Curves. Using the data shown in Figure 3, eq 21 was used to determine $\Delta G'$ at each temperature for each concentration of GdnHCl between 0 and 2 M. Individual unfolded-protein baselines were used in the determination of K_{app} at each temperature for each composite thermal melt, as illustrated in Figure 5. Figure 6a shows data for those concentrations of GdnHCl (0.2−1 M) in which no significant structural unfolding transition is observed at low temperatures, but nevertheless, values for $\Delta G'$ could be determined at low temperatures from the isothermal GdnHCl-induced denaturation curves determined at the low temperatures by linear extrapolation of $\Delta G'$ to

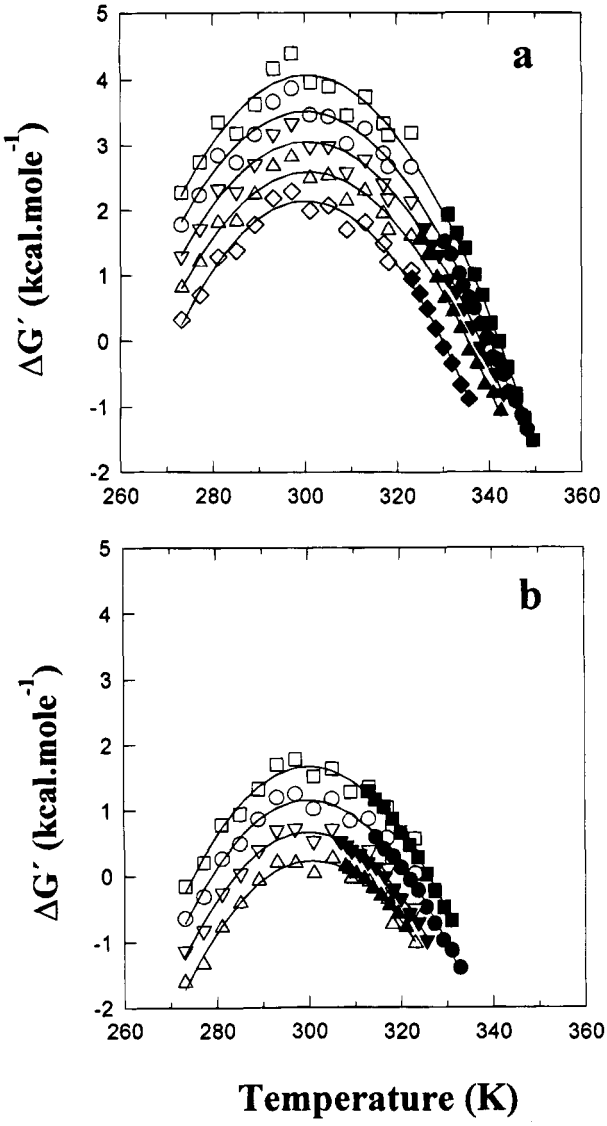

FIGURE 6: Stability curves of barstar at pH 8 in the presence of different concentrations of GdnHCl. The data shown in Figure 3 were used to determine $\Delta G'$ at each temperature for each concentration of GdnHCl between 0 and 2 M, using eq 19. (a) (□) 0.2 M; (○) 0.4 M; (▽) 0.6 M; (△) 0.8 M; (◇) 1.0 M. (b) (□) 1.2 M; (○) 1.4 M; (▽) 1.6 M; (△) 1.8 M. Open and closed symbols are from isothermal GdnHCl-induced denaturation curves and thermally-induced denaturation curves, respectively. For the concentrations of GdnHCl shown in panel a, $\Delta G'$ at low temperatures was obtained from the isothermal GdnHCl-induced denaturation curves determined at these temperatures by linear extrapolation of $\Delta G'$ to the desired concentration of GdnHCl, using eq 5. Each stability curve was analyzed using a nonlinear least squares fit to eq 16, and the values for $\Delta H_g'$, $\Delta S_g'$, $\Delta C_P'$, and T_g' determined for each concentration of GdnHCl are listed in Table 1. To preserve clarity, error bars for the values for $\Delta G'$ have not been shown, but the errors are similar to those indicated for ΔG in the legend to Figure 2a.

the desired concentration of GdnHCl, using eq 5. Figure 6b contains data for those concentrations of GdnHCl (1.2–1.8 M) in which a significant structural unfolding transition is observed at low temperatures (Figure 3). It is observed that $\Delta G'$ becomes equal to 0 at two separate temperatures, corresponding to the low- and the high-temperature melting points. The stability curve ($\Delta G'$ versus T) so determined for each concentration of GdnHCl was analyzed according to eq 16. To determine the values for $\Delta H_g'$, $\Delta S_g'$, $\Delta C_P'$, and T_g', which characterize the heat denaturation process, each stability curve was fit by a nonlinear least squares routine to eq 16 with the sole constraint that $\Delta C_P > 0$. To determine the values of $\Delta H_g^{c\prime}$, $\Delta S_g^{c\prime}$, $\Delta C_P'$, and $T_g^{c\prime}$, which characterize the cold denaturation process, each stability curve was similarly fit to eq 16 with the additional constraint that $\Delta H_g'$ be negative. The thermodynamic parameters obtained are listed in Table 1. Also listed in Table 1 are the values for the other thermodynamic parameters T_s', T_h' and $\Delta G_s'$ that could be determined using eqs 24–26.

There are several points to note regarding the results of the analysis presented in Table 1. (1) The values obtained for T_g' and $T_g^{c\prime}$ are within 0.5 K of the values obtained from visual interpolation of the data in Figure 6 for the two temperatures where $\Delta G' = 0$. In addition, the value obtained for T_g' is within 0.5 K of the value obtained from van't Hoff analysis of only the heat denaturation data (see Materials and Methods). (2) The values obtained for $\Delta C_P'$ from an analysis of the cold denaturation and heat denaturation processes are identical. This result validates the assumption of a temperature-independent ΔC_P over a range of temperature spanning 90 K. (3) The value of ΔG_s, the free energy of unfolding at temperature T_s, where the protein is most stable, decreases with increasing GdnHCl concentration, and at concentrations of GdnHCl greater than 1.8 M, the unfolded state is more stable than the folded state at all temperatures. This is expected because the maximum value of C_m, the midpoint of a GdnHCl-induced denaturation curve, is 1.9 ± 0.1 (Figure 2c). (4) T_s', the temperature at which $\delta\Delta G'/\delta T = 0$, is virtually independent of GdnHCl concentration and has an average value of 300.4 ± 0.5 K.

In Figure 7a is presented a plot of $\Delta H_g'$ versus T_g'. It is observed that T_g' spans a 35 K range in temperature in the presence of GdnHCl. The data fits well to a straight line with a slope of 1510 ± 86 cal mol^{-1} K^{-1}, which represents an apparent $\Delta C_P'$. It should also be observed that the data point representing ΔH_g and T_g agrees well with the fitted line. In Figure 7b is presented a plot of $\Delta C_P'$ versus concentration of GdnHCl. A very small increase (less than 8%) in the value of $\Delta C_P'$ is observed with increasing GdnHCl concentration. The straight line through the data has a slope of 53 ± 36 cal mol^{-1} K^{-1} M^{-1}, which represents ΔC_{Pi}, the change in heat capacity associated with the preferential interaction of GdnHCl with unfolded protein over that with the folded protein (eq 8). It should be noted that this data by itself cannot be used to argue that $\Delta C_P'$ increases, albeit marginally, with an increase in GdnHCl concentration, but the fact that a similar value for ΔC_{Pi} is obtained from the temperature dependencies of ΔH_i (Figure 9a) and ΔS_i (Figure 9b) would support such a conclusion. We consider the average value of ΔC_P = 1460 ± 70 cal mol^{-1} K^{-1} as a good estimate of the true value. It is not very different from the value obtained directly, by fitting the data shown in Figure 2a to eq 4, 1490 ± 50 cal mol^{-1} K^{-1} and also makes allowance for the observed, weak dependence of ΔC_P on GdnHCl concentration.

Evaluation of ΔG_i, ΔH_i, and ΔS_i. The data shown in Figure 6 were used for a detailed analysis of the dependencies of $\Delta H'$, $\Delta S'$, and $\Delta C_P'$ on the concentration of GdnHCl. For any concentration of GdnHCl, the values for $\Delta H'$, $\Delta S'$, and $\Delta G'$ at any temperature could be determined using eqs 14–16 in conjunction with the values for $\Delta H_g'$, $\Delta S_g'$, T_g', and $\Delta C_P'$ listed in Table 1. In Figure 8, panels a and b, are shown the dependencies of $\Delta H'$ and $\Delta S'$ on the concentration of

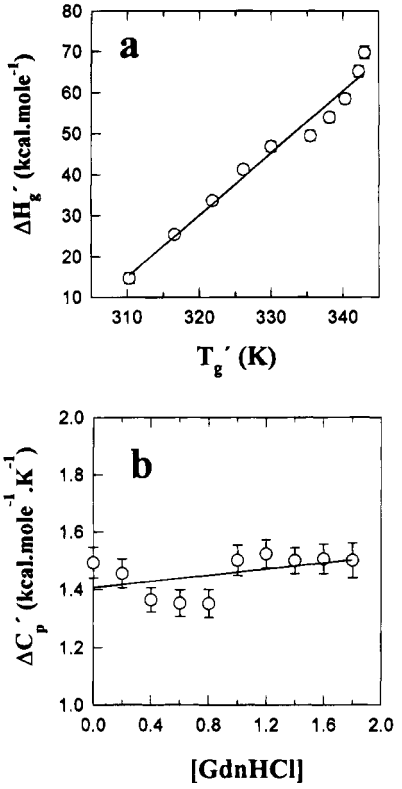

FIGURE 7: ΔC_P of unfolding of barstar at pH 8. (a) Dependence of $\Delta H_g'$ on T_g'. The value of $\Delta H_g'$ determined at each temperature T_g', which was varied by changing the concentration of GdnHCl present (see Table 1), is plotted against T_g'. The slope of the linear least squares fitted line through the data, which represents an apparent ΔC_P, has a value of 1510 ± 86 cal mol^{-1} K^{-1}. (b) Dependence of $\Delta C_P'$ on GdnHCl concentration. $\Delta C_P'$ is plotted against GdnHCl concentration, using the values listed in Table 1. The solid line through the data is a linear least squares fit of the data to eq 8. The slope and intercept of the line, representing ΔC_{Pi} and ΔC_P, respectively, have values of 53 ± 36 cal mol^{-1} K^{-1} M^{-1} and 1410 ± 40 cal mol^{-1} K^{-1}. The error bars in (a) and (b) represent the standard errors determined from nonlinear least squares analysis of the stability curves in Figure 6 to eq 13. The standard error in the determination of T_g' is less than ±0.5 K.

GdnHCl at two different temperatures, 273 and 317 K. At 273 K, $\Delta H'$ has a negative value whose magnitude increases linearly with increasing GdnHCl concentration, indicating a favorable interaction of GdnHCl with barstar at this low temperature (Figure 8a). $\Delta S'$ too is a negative quantity at this temperature, and its absolute value also increases with increasing GdnHCl concentration (Figure 8b). The values of $\Delta H'$ and $\Delta S'$ at any particular temperature and GdnHCl concentration are such that the resultant value of $\Delta G'$ decreases linearly with increasing GdnHCl concentration (Figure 8c). Figure 8c also shows data for $\Delta G'$ at 297 K for ready comparison with the $\Delta G'$ values at two extremes of temperature. The data in Figure 8a–c were fitted to eqs 5–7. The slopes and intercepts of the fitted straight lines in Figure 8a–c yield the values for ΔH and ΔH_i, ΔS and ΔS_i, and ΔG and ΔG_i, respectively, which are listed in the legend to Figure 8. Data for two different temperatures covering the temperature range of isothermal GdnHCl-induced denaturation curves have been shown to give the reader an appreciation of the errors involved in the determination of these parameters. It should be noted that the values obtained for ΔG from these linear fits agree well with the values obtained directly for these parameters, which are also shown in Figure 8c.

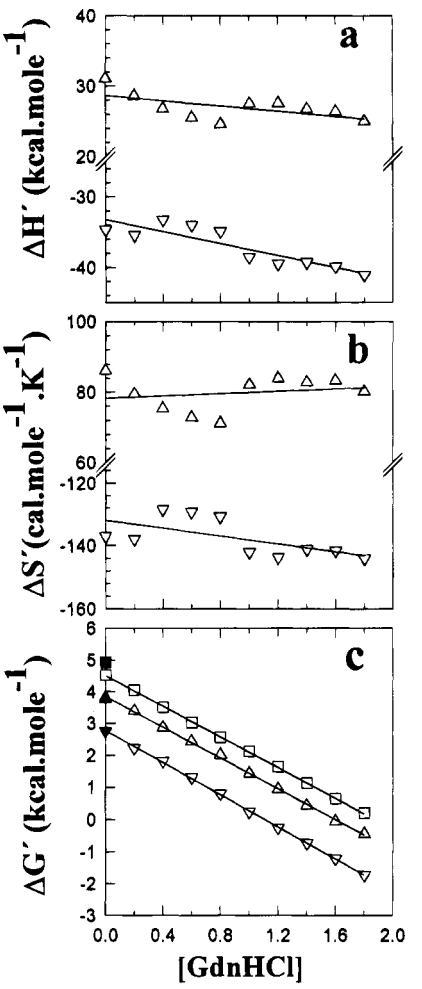

FIGURE 8: GdnHCl concentration dependencies of $\Delta H'$, $\Delta S'$, and $\Delta G'$ at pH 8. The values for $\Delta H'$, $\Delta S'$, and $\Delta G'$ were determined at three different temperatures 273 (▽), 297 (□), and 317 K (△) for each concentration of GdnHCl using eqs 14–16 and the values for $\Delta H_g'$, $\Delta S_g'$, T_g', and $\Delta C_P'$ listed in Table 1. The dependencies of (a) $\Delta H'$ and (b) $\Delta S'$ (only at 273 and 317 K) and (c) $\Delta G'$ (at 273, 317, and 297 K) on the concentration of GdnHCl are shown. In c, the filled symbols denote the values of ΔG determined from an analysis of GdnHCl-induced denaturation curves obtained at the corresponding temperatures. The straight lines through the data in a–c are linear least squares fits of the data to eqs 6, 7, and 5, respectively. The slopes and intercepts of the fitted lines yield the values for ΔH, ΔH_i, ΔS, ΔS_i, ΔG, and ΔG_i of −33.3 ± 0.8 kcal mol^{-1}, −4.21 ± 0.8 kcal mol^{-1} M^{-1}, −131.9 ± 2.9 cal mol^{-1} K^{-1}, −6.3 ± 2.7 cal mol^{-1} K^{-1} M^{-1}, 2.8 ± 0.02 kcal mol^{-1}, and −2.5 ± 0.02 kcal mol^{-1} M^{-1}, respectively, at 273 K and 28.7 ± 0.9 kcal mol^{-1}, −1.9 ± 0.9 kcal mol^{-1} M^{-1}, 78.3 ± 3.1 cal mol^{-1} K^{-1}, 1.63 ± 2.9 cal mol^{-1} K^{-1} M^{-1}, 3.8 ± 0.03 kcal mol^{-1}, and −2.4 ± 0.03 kcal mol^{-1} M^{-1}, respectively, at 317 K. At 297 K, the ΔG and ΔG_i values are 4.5 ± 0.02 kcal mol^{-1} and −2.4 ± 0.01 kcal mol^{-1} M^{-1}.

An analysis similar to that shown in Figure 8 was carried out at each of 13 different temperatures in the range 273–321 K, and the values of ΔH_i, ΔS_i, and ΔG_i were determined at each temperature. Figure 9, panels a–c, shows the temperature dependencies of ΔH_i, ΔS_i, and ΔG_i. ΔH_i becomes more negative with decreasing temperature. The slope of the straight line through the plot of ΔH_i versus T, according to eq 11, is equal to ΔC_{Pi} and has a value of 53 ± 36 cal mol^{-1} K^{-1} M^{-1}, which is similar to the mean value determined from the data in Figure 7b. The straight line extrapolates to $\Delta H_i = 0$ at 353 K, above which ΔH_i makes an unfavorable contribution to ΔG_i. ΔS_i has a negative value

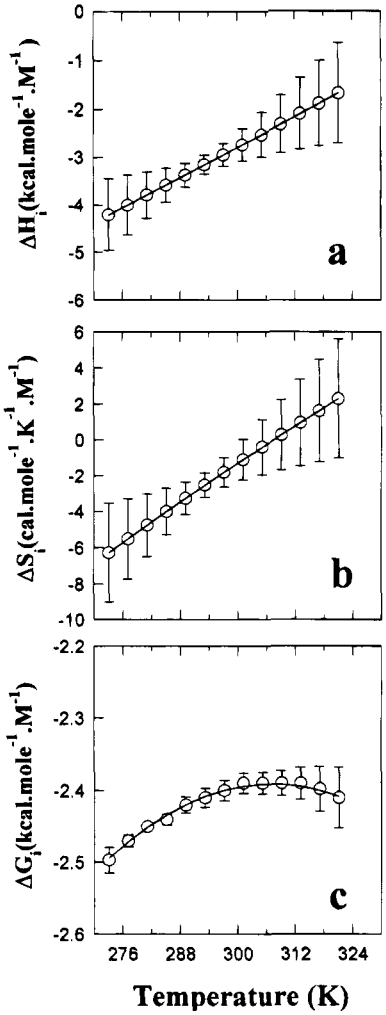

FIGURE 9: Temperature dependence of the thermodynamic parameters governing the interaction of barstar with GdnHCl at pH 8. (a) Dependence of ΔH_i. The straight line through the data is a linear weighted least squares fit of the data to eq 11, whose slope is equal to ΔC_{Pi} and has a value of 53 ± 36 cal mol^{-1} K^{-1} M^{-1}. (b) Dependence of ΔS_i. The line through the data is a weighted least squares fit to eq 12, which gives a value for ΔC_{Pi} of 53 ± 36 cal mol^{-1} K^{-1} M^{-1}. (c) Dependence of ΔG_i. The solid line through the data is drawn according to eq 10, with the fitted values of ΔH_i and ΔS_i at each temperature obtained as described above. The errors shown in the values for ΔH_i, ΔS_i, and ΔG_i are the standard errors obtained from least squares fits as shown in Figure 8.

at low temperatures, but the value becomes more positive with increasing temperature, so that $\Delta S_i = 0$ at 308 K above which is makes a favorable contribution to ΔG_i (Figure 9b). ΔG_i, determined as the slope of a plot of $\Delta G'$ versus GdnHCl concentration (Figure 8c), is seen to have a small dependence on temperature. It appears that the value of ΔG_i goes through a maximum with increasing temperature, as expected from eq 13. Moreover, the values of ΔH_i and ΔS_i at each temperature could be used in eq 10 to correctly predict the temperature dependence of ΔG_i as shown in Figure 9c.

GdnHCl Concentration Dependence of T_g', $T_g^{c'}$, T_h', and T_s'. Figure 10a shows the GdnHCl concentration dependence of T_g' and $T_g^{c'}$. The former decreases with increasing GdnHCl concentration, while the latter increases, and they both appear to converge to the same value of 300 K at 1.9 M GdnHCl. Figure 10a also shows that the values obtained for $T_g^{c'}$ from an analysis of the stability curves in Figure 6 agree well with the values predicted by eq 27. Figure 10b shows the dependencies of T_h' and T_s' on the concentration

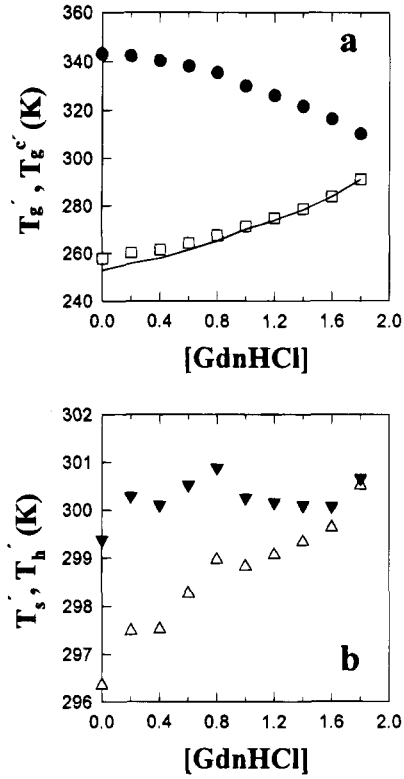

FIGURE 10: GdnHCl concentration dependencies of T_h', T_s', T_g', and $T_g^{c'}$ for barstar at pH 8. (a) Dependencies of T_g' (●) and $T_g^{c'}$ (□). (b) Dependencies of T_h' (△) and T_s' (▼). The values for all four characteristic temperatures are listed in Table 1. The solid line through the $T_g^{c'}$ data is drawn according to eq 27, using the values for $\Delta H_g'$, $\Delta C_P'$, and T_g' listed in Table 1.

of GdnHCl. The former increases in value, while the latter remains more or less constant with an increase in GdnHCl concentration. In approximately 1.9 M GdnHCl, T_h' and T_s' have the same value of 300 K. Thus, in 1.9 M GdnHCl, T_g' = $T_g^{c'}$ = T_h' = T_s' = 300 K. It should be noted that T_h' = T_s' only when $\Delta G = 0$ and $\delta\Delta G/\delta T = 0$, i.e., when K_{eq} = 1. This is indeed the case in 1.9 M GdnHCl and 300 K, where the fully folded and unfolded states do not differ in enthalpy ($\Delta H' = 0$), entropy ($\Delta S' = 0$), or consequently in free energy ($\Delta G' = 0$).

DISCUSSION

Cold Denaturation. The phenomenon of cold denaturation of proteins is by now a well-accepted fact. After the original prediction by Brandts (Brandts, 1964), several proteins have been shown to undergo such transitions [reviewed by Privalov (1990)]. Most proteins that undergo cold denaturation do so under conditions where the native state of the protein is already destabilized either by the presence of a denaturant or extremes of pH (Privalov, 1990). The study of the thermodynamics of cold denaturation is facilitated by the presence of a denaturant because the denaturant raises the cold transition temperature, allows faster equilibration, and depresses the freezing point of water, preventing ice formation (Becktel & Schellman, 1987; Chen & Schellman, 1989). Previously, cold denaturation of small proteins in the presence of denaturants has been reported in the case of β-lactoglobulin (Christensen, 1952; Pace & Tanford, 1968), cytochrome *c*-552 (Nojima *et al.*, 1978), myoglobin (Privalov *et al.*, 1986), staphylococcal nuclease (Griko *et al.*, 1988),

and a mutant form of T4 lysozyme (Chen & Schellman, 1989). This is the first paper describing the cold denaturation of barstar.

The data in Figures 1−3 and 6 indicate that barstar undergoes a decrease in stability as the temperature is lowered below 300 K. The decrease in stability at low temperatures, observed in the presence of denaturants (Figure 6), can be explained in part by the increase in the enthalpy of interaction of GdnHCl with the protein at low temperatures: ΔH_i becomes increasingly negative with decreasing temperature (Figure 9) and makes an increasingly favorable contribution to ΔG_i (eq 10) and, consequently, to $\Delta G'$ (eq 5). As expected from eq 5, the stability decreases when the concentration of GdnHCl is increased (Figure 6). When the concentration of GdnHCl is less than 1.0 M, the decrease in stability is not sufficient for a significant structural unfolding transition to be seen by either far- or near-UV CD (see Figure 1), but if the GdnHCl concentration is greater than 1.2 M, a structural unfolding transition is seen at low temperatures (Figure 3).

Figures 1 and 2 and Table 1 show that regardless of whether GdnHCl is present or not, the decrease in stability at high temperatures proceeds with an overall increase in enthalpy and entropy, while the decrease in stability at low temperatures (below T_s) proceeds with an overall decrease in both enthalpy and entropy. It is clear that in the absence of GdnHCl, the folded protein molecule cannot possess higher conformational entropy (disorder) than the cold-denatured protein molecule. The change in the entropy of water must therefore be making a substantial contribution to the observed decrease in entropy that accompanies cold denaturation. The source of this change in the entropy of water must be the hydrophobic effect (Kauzmann, 1959), which must therefore be the dominant force stabilizing barstar. The hydrophobic effect decreases with decreasing temperature (Kauzmann, 1959; Privalov & Gill, 1988), and this may be a principal reason why the stability of barstar decreases with decreasing temperature at temperatures below T_s. The contribution of the hydrophobic effect to protein denaturation and to cold denaturation in particular has been described by Privalov (1989, 1990, 1992).

The enthalpy of cold-denatured barstar also cannot be lower than that of the folded protein, because that would mean that cold-denatured barstar has more structure than the folded state. Thus, the change in the enthalpy of interaction of water with the protein must be making a substantial contribution to the observed decrease in enthalpy that accompanies cold denaturation (Privalov, 1990).

The data in Table 1 indicate that in the presence of intermediate concentrations of GdnHCl, in the range 1.2−2.0 M, barstar is in the cold-denatured state at 273 K. As the temperature is increased from 273 K, the protein first absorbs heat to refold around temperature $T_g^{c\prime}$, reaches a state of maximum stability at a temperature T_s', and then absorbs heat to unfold to the heat-denatured state around temperature T_g'. The overall transition from the cold-denatured state to the heat-denatured state is not accompanied by a change in heat capacity: the heat capacities of the cold- and heat-denatured states are identical.

Prediction of Observable Cold Denaturation. Barstar has an unusually high value of ΔC_P for a protein its size. The value of 1460 cal mol^{-1} K^{-1} translates into a value of 16.4 cal mol^{-1} K^{-1} per residue. Only myoglobin has a higher value, that of 18 cal mol^{-1} K^{-1} per residue while the values for ribonuclease A, ribonuclease T1, lysozyme, barnase, and staphylococcal nuclease fall in the range 12−15 cal mol^{-1} K^{-1} per residue (Privalov, 1992). What is most unusual about barstar is that it has an unusually low value for ΔH of only 4.0 ± 0.2 kcal mol^{-1} at 298 K compared to the values reported for ribonuclease A (Makhatadze & Privalov, 1992), ribonuclease T1 (Pace & Laurents, 1989), lysozyme (Makhatadze & Privalov, 1992), barnase (Griko *et al.*, 1994), and staphylococcal nuclease (Antonino *et al.*, 1991), which fall in the range 25−75 kcal mol^{-1} at the same temperature. Myoglobin too has an abnormally low value for ΔH of 7.8 kcal mol^{-1} at 298 K (Privalov, 1992). It is therefore not surprising that myoglobin too undergoes an observable cold denaturation reaction (Privalov *et al.*, 1986) because it has an unusually low value for $\Delta H_g/\Delta C_P$, as does barstar. According to eq 27, a low value of $\Delta H_g/\Delta C_P$ predicts that cold denaturation will fall within an observable temperature range.

Interaction of Denaturants with Proteins. In spite of a very large number of investigations that utilize chemical denaturants such as urea and GdnHCl to unfold proteins, the actual mechanism by which solvent denaturation occurs is still poorly understood. Two models are generally used to quantitatively analyze solvent denaturation. According to the binding model (Tanford, 1970; Lee & Timasheff, 1974), denaturants bind stoichiometrically to proteins, but there is very little experimental evidence for stoichiometric binding. According to the linear free energy model, which was first used empirically by Greene and Pace (1974) but later given a theoretical basis by Schellman (1978, 1987), denaturants display many, weak, selective interactions with proteins. The premise of either model is that the denaturant interacts preferentially with the unfolded form of the protein in comparison to the folded form. In the binding model, the larger number of binding sites available in the unfolded form accounts for the preferential interaction, while in the linear free energy model, the larger solvent-accessible surface area of the unfolded form accounts for the preferential interaction. Experimentally, the two models are distinguished by the former postulating a logarithmic dependence of the free energy of unfolding ($\Delta G'$) on denaturant concentration, and the latter postulating a linear dependence. The unfolding of proteins by denaturants has also been modeled on the free energy of transfer of the individual amino acids from a nonpolar to polar solvent (Tanford, 1970; Pace 1986), and it has been shown that the free energy of transfer to denaturant solutions is linearly dependent on the concentration of the denaturant (Tanford, 1970). Thus, it is not surprising that the free energy of unfolding is usually observed to possess a linear dependence on the concentration of denaturant.

Determination of ΔC_P. The analysis of the stability curves of barstar determined in the presence of fixed concentrations of GdnHCl in the range 0−2 M yield unusually precise appraisals of $\Delta C_P'$ because the slope of each stability curve changes from a large positive value to a large negative value with an increase in temperature. The good fits of the data in Figure 6 to eq 16 and the demonstration that the same value for ΔC_P is obtained from separate analyses of the cold and heat denaturation segments of the stability curves (see Results) therefore provide a rigorous validation of the assumption that the change in heat capacity is independent

of temperature, in the temperature range under consideration (Chen & Schellman, 1989).

There are many reports in the literature of using chemical denaturants to alter T_g and then determining the value of ΔC_P as the slope of the resultant $\Delta H_g'$ versus T_g' plot (Santoro & Bolen, 1992). The $\Delta H_g'$ values need to be corrected for the enthalpy of association of the denaturant with the protein so as to obtain ΔH_g values, and it is the slope of the resultant ΔH_g versus T_g plot that yields the correct value of ΔC_P (Privalov, 1979). Nevertheless, it should be noted that the apparent value obtained for ΔC_P from a plot of $\Delta H_g'$ versus T_g' plot usually falls within the 10% error that is usually present in the determination of the true value of ΔC_P from a ΔH_g versus T_g plot. For example, the plot of $\Delta H_g'$ versus T_g' for barstar, using data presented in Table 1, yields an apparent value for ΔC_P of 1510 ± 86 cal mol^{-1} K^{-1} (Figure 5a), which is almost the same as the true value of 1460 ± 70 cal mol^{-1} K^{-1} determined after accounting for the enthalpy of interaction with GdnHCl.

The data in Figures 7b and 9a indicate that the value of $\Delta C_P'$ increases, albeit to a small extent, with an increase in the concentration of GdnHCl. Earlier reports present a conflicting picture of the effect of denaturant on $\Delta C_P'$. No clear trend was observed in the case of urea denaturation of β-lactoglobulin (Pace & Tanford, 1968; Griko & Privalov, 1992), but later studies showed that a two-state unfolding transition was not applicable in this case (Tanford, 1970). Calorimetric studies have indicated that the value of $\Delta C_P'$ is higher in the presence of chemical denaturants (Pfeil & Privalov, 1976; Makhatadze & Privalov, 1992) for the unfolding of both ribonuclease A and lysozyme, but the trend is more clear in the case of GdnHCl-induced denaturation than in the case of urea-induced denaturation. There is also a report of ΔC_P being lowered in the presence of chemical denaturants (Kreschek & Benjamin, 1964).

Validation of the Linear Free Energy Model. The determination of $\Delta H_g'$, T_g', and $\Delta C_P'$ from the stability curves obtained in the presence of different concentrations of GdnHCl in the range 0.2−1.0 M made it possible to determine the value of $\Delta G'$ at each concentration of GdnHCl at different temperatures by the use of eq 16 (Pace & Laurents, 1989). Figure 8c shows the results of doing this for the data at 273, 297, and 317 K. The slope of the plot of $\Delta G'$ versus GdnHCl concentration yields the value of m_G, and the y axis intercept yields the value of ΔG at the mentioned temperatures. It is seen that the value for ΔG as well as the value for m_G obtained from such a plot are similar to the values obtained directly from a GdnHCl-induced denaturation curve (Figure 2) obtained at 273, 297, and 317 K. It should be noted that the determination of ΔG at either 273 or 317 K as illustrated in Figure 8c involves a relatively short linear extrapolation of $\Delta G'$ values because the lower stability of barstar at extremes of temperature results in a lower value of C_m. In contrast, determination of ΔG from the GdnHCl-induced denaturation curve obtained at 297 K involves a longer linear extrapolation of $\Delta G'$ values determined within the transition zone (1.4−2.6 M). The good agreement between the two values for ΔG seen in Figure 8c authenticates the use of linear extrapolation of ΔG values determined within the transition zone to determine ΔG, which is the conventional procedure in measurements of protein stability (Pace, 1986). In Figure 9c, the temperature dependence of ΔG_i (m_G) determined as described in Figure 8c is plotted. The value obtained for m_G at each temperature is the same, within experimental error, as the value obtained directly from the GdnHCl-induced denaturation curve determined at that temperature (Figure 2b).

The ability to predict the value of ΔG_i from the values of ΔH_i and ΔS_i at any temperature (Figure 9) and the demonstration that the predicted value is the same, within experimental error, as the experimentally observed value (Figure 2b) validate the use of linear extrapolation to determine the ΔG values from GdnHCl-induced unfolding data. It should be mentioned that the validity of the linear free energy model for analyzing the stability of barstar had earlier been indicated by the result that the same value for ΔG is obtained at pH 7 (4.9 ± 0.4 kcal mol^{-1}) when the model is used for the analysis of both urea-induced and GdnHCl-induced denaturation curves (R. Khurana and J. B. Udgaonkar, unpublished results).

Thermodynamics of the Interaction between Barstar and GdnHCl. Figures 2, 7, and 8 show that the linear free energy model can fully account for the interaction of GdnHCl with barstar. The value of m_G, the dependence of the stabilization free energy on GdnHCl concentration, appears not to change even when the value of C_m (and consequently, the range of GdnHCl concentration in which barstar unfolds) is varied 2-fold by varying the temperature (Figure 2). Figure 8 shows that all three thermodynamic parameters, $\Delta H'$, $\Delta S'$, and $\Delta G'$ have a linear dependence on GdnHCl concentration as demanded by the linear free energy model.

Temperature Dependence of m_G. According to the linear free energy model of Schellman (1978), m_G represents the excess free energy of interaction of GdnHCl with the unfolded protein in comparison to the folded protein. It is therefore expected, according to eq 13, to be dependent on temperature. The data in Figure 2b suggest, however that in the case of barstar m_G is independent within experimental error of temperature in the range 273−323 K. Similarly, in the case of both ribonuclease T1 (Hu *et al.*, 1992) and a mutant form of T4 lysozyme (Chen & Schellman, 1989), m_G has been observed to be apparently independent of temperature over a 30 K range. In neither of these two cases was the apparent temperature independence explained.

At least in the case of barstar, the apparent temperature independence of m_G that is observed over a 50 K range in temperature (Figure 2b) is because of the very small value of ΔC_{Pi} (53 ± 36 cal mol^{-1} K^{-1} M^{-1}). This results in a very small curvature in a plot of ΔG_i versus T, and consequently, ΔG_i appears to be independent of temperature in the range of temperatures between 273 and 323 K. The preferential enthalpy (ΔH_i) of interaction of GdnHCl with the unfolded state than with the folded state is large and favorable at low temperatures (Figure 9a). The stabilizing contribution of ΔH_i to ΔG_i is, however, opposed by the destabilizing contribution of the $T\Delta S_i$ term to ΔG_i (eq 10). At low temperatures, ΔS_i is negative because the GdnHCl molecules are immobilized in the vicinity of the protein molecules. With increasing temperature, the contribution of ΔS_i becomes less destabilizing, and above 308 K, it becomes stabilizing (Figure 9b). The stabilizing contribution of ΔH_i however becomes less favorable with increasing temperature. With an increase in temperature, the interaction enthalpy and entropy compensate each other in such a manner that the change in the value of ΔG_i is within the error of experimental determination.

In the most detailed study so far of the interaction of denaturants with proteins, done using calorimetric methods (Makhatadze & Privalov, 1992), the analysis was done on the basis of the binding model (Tanford, 1970). In that study, the binding enthalpy of GdnHCl was approximately −10 to −12 kcal mol^{-1} in 1.0 M GdnHCl at 297 K for both ribonuclease A and lysozyme (Makhatadze & Privalov, 1992; Pfeil & Privalov, 1976). In contrast, the binding enthalpy for the binding of GdnHCl to barstar at 297 K is determined here, by use of the linear free energy model, to be approximately −3 kcal mol^{-1} (Figure 9a), indicating that GdnHCl interacts less favorably with barstar than with ribonuclease A or lysozyme. Although the binding model could be successfully applied to analyze the interaction of GdnHCl and urea with ribonuclease A and lysozyme, as studied by both scanning calorimetry and isothermal titration calorimetry, the deviations from linearity of the dependencies of values of $\Delta G'$ on denaturant concentration were small (Makhatadze & Privalov, 1992), and other models could not be ruled out. In the case of barstar too, although the linear free energy model predicts and accounts for all the data, it is possible that other models might also satisfactorily account for the data.

Structure in Thermally Unfolded Barstar. It has been observed in the case of several proteins (Robertson & Baldwin, 1991; Evans *et al.*, 1991), including barstar (Khurana & Udgaonkar, 1994), that the mean residue ellipticity at 222 nm of the thermally unfolded protein is more than that of the protein unfolded in 6 M GdnHCl. This observation has usually been taken as evidence for residual structure in thermally unfolded protein that disappears on further unfolding by GdnHCl. The data in Figure 4 indicate that although in the absence of GdnHCl barstar appears to possess some residual secondary structure when thermally unfolded, this structure is not removed by GdnHCl in a cooperative manner. This suggests that the reduction in mean residue ellipticity with increasing GdnHCl concentration seen in Figure 4 does not actually represent a structural transition and certainly does not represent a cooperative structural transition. Supportive of this observation are the results of several calorimetric studies (Pfeil & Privalov, 1976; Privalov, 1979), which have failed to detect any thermodynamic transition on the titration of thermally unfolded proteins with chemical denaturants. It appears that the mean residue ellipticity of an unfolded protein depends on both the temperature and the concentration of GdnHCl in a linear manner and that no cooperative transition occurs on changing either variable. This has been observed for other proteins (Pace & Tanford, 1968; Nojima *et al.*, 1978; Privalov *et al.*, 1989) and is seen here for barstar (Figures 3 and 5). It is possible that the transition instead represents gradual structural changes in the conformation of the unfolded protein, which have been rationalized by Dill and Shortle (1991).

A study of the cold denaturation of barstar using differential scanning calorimetry and a structural characterization of the cold-denatured state by other spectroscopic methods are also in progress. Interestingly, barstar has an unusually low value for ΔH at 298 K and, consequently, an unusually low value for ΔS (see above). Recently, there have been several attempts at correlating the thermodynamic parameters that define the stability of a protein to its amino acid sequence and structure (Spolar *et al.*, 1992; Privalov & Makhatadze, 1993; Makhatadze & Privalov, 1993; Griko *et al.*, 1994; Yu *et al.*, 1994). The correlation between the thermodynamic parameters to sequence and structure parameters is currently being studied.

In summary, this paper describes the thermodynamics of two different processes. It is the first paper describing the cold denaturation of barstar, and the thermodynamics of the cold and heat denaturation processes have been characterized in detail. The ability to study both heat and cold denaturation over a wide range of GdnHCl concentration has made it possible to determine the thermodynamic parameters $\Delta H'$, $\Delta S'$, $\Delta G'$, and $\Delta C_P'$ in the presence of GdnHCl with unusually high precision. This in turn has made it possible to determine the changes in enthalpy, entropy, free energy, and heat capacity that accompany the preferential interaction of GdnHCl with the unfolded form of barstar with respect to the folded form. The linear free energy model is the model most commonly used to analyze chemical denaturant-induced denaturation curves. The theoretical basis of this model was proposed several years ago (Schellman, 1978), and in this paper an evaluation of all the thermodynamic parameters that define the model has been carried out in the case of barstar, and the validity of the linear free energy model was clearly established.

ACKNOWLEDGMENT

We thank Raghavan Varadarajan for his comments on the manuscript.

REFERENCES

Antonino, L. C., Kautz, R. A., Nakano, T., Fox, R. O., & Fink, A. L. (1991) *Proc. Natl. Acad. Sci. U.S.A. 88*, 7715−7718.
Becktel, W. J., & Schellman, J. A. (1987) *Biopolymers 26*, 1869−1877.
Brandts, J. F. (1964) *J. Am. Chem. Soc. 86*, 4291−4314.
Buckle, A. M., Schreiber, G., & Fersht, A. R. (1994) *Biochemistry 33*, 8878−8889.
Chen, B. L., & Schellman, J. A. (1989) *Biochemistry 28*, 685−691.
Christensen, J. K. (1952) *C. R. Trav. Lab. Carlsberg, Ser. Chim. 28*, 37−169.
Dill, K. A., & Shortle, D. (1991) *Annu. Rev. Biochem. 60*, 795−825.
Evans, P. A., Topping, K. D., Woolfson, D. N., & Dobson, C. M. (1991) *Proteins: Struct. Funct. Genet. 9*, 248−266.
Greene, R. F., & Pace, C. N. (1974) *J. Biol. Chem. 249*, 5388−5393.
Griko, Y. V., & Privalov, P. L. (1992) *Biochemistry 31*, 8810−8815.
Griko, Y. V., Privalov, P. L., Sturtevant, J. M., & Venyaminov, S. Y. (1988) *Proc. Natl. Acad. Sci. U.S.A. 85*, 3343−3347.
Griko, Y. V., Makhatadze, G. I., Privalov, P. L., & Hartley, R. W. (1994) *Protein Sci. 3*, 669−676.
Guillet, V., Lapthorn, A., Hartley, R. W., & Mauguen, Y. (1993) *Structure 1*, 165−176.
Hartley, R. W. (1988) *J. Mol. Biol. 202*, 913−915.
Hu, C.-Q., Sturtevant, J. M., Thomson, J. A., Erickson, R. E., & Pace, C. N. (1992) *Biochemistry 31*, 4876−4882.
Kauzmann, W. (1959) *Adv. Protein Chem. 14*, 1−63.
Khurana, R., & Udgaonkar, J. B. (1994) *Biochemistry 33*, 106−115.
Kreschek, G. C., & Benjamin, L. (1964) *J. Phys. Chem. 68*, 2476−2486.
Lee, J. C. & Timasheff, S. N. (1974) *Biochemistry 13*, 257−265.
Lubienski, M. J., Bycroft, M., Jones, D. N. M., & Fersht, A. R. (1993) *FEBS Lett. 332*, 81−87.

Lubienski, M. J., Bycroft, M., Freund, S. M. V., & Fersht, A. R. (1994) *Biochemistry 33*, 8866−8877.
Makhatadze, G. I., & Privalov, P. L. (1992) *J. Mol. Biol. 226*, 491−505.
Makhatadze, G. I., & Privalov, P. L. (1993) *J. Mol. Biol. 232*, 639−659.
Nojima, H., Honnami, K., Oshima, T., & Noda, H. (1978) *J. Mol. Biol. 122*, 33−42.
Pace, C. N. (1986) *Methods Enzymol. 131*, 266−280.
Pace, C. N., & Tanford, C. (1968) *Biochemistry 7*, 198−20.
Pace, C. N., & Laurents, D. V. (1989) *Biochemistry 28*, 2520−2525.
Pfeil, W., & Privalov, P. L. (1976) *Biophys. Chem. 44*, 33−40.
Privalov, P. L. (1979) *Adv. Protein Chem. 33*, 167−241.
Privalov, P. L. (1989) *Annu. Rev. Biophys. Biophys. Chem. 18*, 47−69.
Privalov, P. L. (1990) *Crit. Rev. Biochem. Mol. Biol. 25*, 281−305.
Privalov, P. L. (1992) in *Protein Folding* (Creighton, T.E., Ed.) pp 83−126, W. H. Freeman & Co., New York.
Privalov, P. L., & Gill, S. J. (1988) *Adv. Protein Chem. 39*, 191−233.
Privalov, P. L., & Makhatadze, G. I. (1993) *J. Mol. Biol. 232*, 660−679.
Privalov, P. L., Griko, Y. V., & Venyaminov, S. Y. (1986) *J. Mol. Biol. 190*, 487−498.
Privalov, P. L., Tiktopulo, E. I., Venyaminov, S. Y., Griko, Y. V., Makhatadze, G. I., & Kechinashvili, N. N. (1989) *J. Mol. Biol. 205*, 737−750.
Robertson, A. D., & Baldwin, R. L. (1991) *Biochemistry 30*, 9907−9914.
Santoro, M. M., & Bolen, D. W. (1988) *Biochemistry 27*, 8063−8068.
Santoro, M. M., & Bolen, D. W. (1992) *Biochemistry 31*, 4901−4907.
Schellman, J. A. (1978) *Biopolymers 7*, 1305−1322.
Schellman, J. A. (1987) *Annu. Rev. Biophys. Biophys. Chem. 16*, 115−137.
Schreiber, G., & Fersht, A. R. (1993) *Biochemistry 32*, 11195−11203.
Shastry, M. C. R., Agashe, V. R., & Udgaonkar, J. B. (1994) *Protein Sci. 3*, 1409−1417.
Shortle, D., Meeker, A. K., & Freire, E. (1988) *Biochemistry 27*, 4761−4768.
Spolar, R. S., Livingstone, J. R., & Record, M. T. (1992) *Biochemistry 31*, 3947−3955.
Swaminathan, R., Periasamy, N., Udgaonkar, J. B., & Krishnamoorthy, G. (1994) *J. Phys. Chem. 98*, 9270−9278.
Tanford, C. (1970) *Adv. Protein Chem. 21*, 1−95.
Yu, Y., Makhatadze, G. I., Pace, C. N., & Privalov, P. L. (1994) *Biochemistry 33*, 3312−3319.

BI9424095